μ Synthesis of Flexible Rotor-Magnetic Bearing Systems

Kenzo Nonami and Takayuki Ito

Abstract— **The μ synthesis design method was evaluated for a flexible rotor magnetic bearing system with a five-axis-control system using both simulations and experiments. After modeling the full-order system using the finite element method, we obtained a reduced-order model in the modal domain by truncating the flexible modes. After choosing appropriate weighting functions with respect to frequency, we designed the μ-synthesis control system using the μ-toolbox in MATLAB. We then carried out simulations of the control system for a flexible rotor magnetic bearing system with a five-axis-control system and obtained good performance. Next, we conducted experiments to verify the robustness of the controllers on a test rig during initial levitation. The μ controllers provided robust stability and performance over a wide range of parameter variations in the test rig.**

I. Introduction

ACTIVE magnetic bearings (AMB's) use electromagnetic force to provide noncontact support for rotors in high-speed rotating machinery. When applied to a rotor systems, magnetic bearings have the advantage of being contactless, of allowing high speed rotation and providing active vibration control. It is therefore necessary to use an asymptotically stable and robust controller for magnetic bearing to support rotor systems. Most controllers in use today were designed using proportional-integral-derivative (PID) strategy. However, it is not easy to satisfy the requirements for robust performance using PID control. Of course, modern control theory for multi-input and multioutput (MIMO) systems can be applied to magnetic bearing systems as a form of advanced control. However, modern control theory cannot treat the uncertainty inherent in the mathematical models used to design control systems. Thus, robust control theory has attracted considerable attention for designing systems to control magnetic bearings [1]–[12].

The μ synthesis method may be used to design controllers that provide robust stabilities and performance. Unfortunately, μ synthesis involves an iterative and nonconvex numerical procedure known as D-K iteration [3], [4].

Previously Fujita *et al.* obtained good experimental results for a flexible beam magnetic suspension system [14]. Fujita *et al.* also presented the very similar research work for a magnetic bearing system [15]. Their control system design approach is also very similar to that presented in this paper. Though the results of Fujita *et al.* show almost the same performance for the H_∞ controller and μ controller, the results of our experiments show drastically different performance. The μ controller exhibits significantly greater robustness to mass variations than the H_∞ controller. It seems that the strong robustness is caused by the high gain of the μ controller in the lower frequency range.

In this paper, μ synthesis is applied to a flexible rotor-magnetic bearing system to examine its performance robustness and to compare it to that of H_∞ control. We obtained excellent results with D-K iteration and found that the static stiffness of the magnetic bearing increases with each successive D-K iteration. Tests were also conducted to determine the stability robustness of the controllers with respect to added rotor mass. Successful rotor levitation was achieved up to a 29% mass increase for the H_∞ controller, while the μ synthesis controller could levitate with up to a 73% variation.

II. Modeling of Flexible Rotor-Magnetic Bearing Systems

The dynamics of the flexible rotor magnetic bearing system will be described in this section. For simplicity, the analysis is performed only in the X direction and all the coupling effects among the different axes and noncollocation are ignored. For the test rig considered, the rotor can be modeled using seven mass stations, as shown in Fig. 1.

A. Flexible Rotor Dynamics

The 14th-order model is obtained using the finite element method as follows:

$$M_0\ddot{q} + K_0 q = 0 \tag{1}$$

where $q = [x_1\theta_1 x_2\theta_2 x_3\theta_3 x_4\theta_4 x_5\theta_5 x_6\theta_6 x_7\theta_7]^T$ and x_i, θ_i $(i = 1, \cdots, 7)$ represent the displacement and angle of mass stations of the rotor, respectively, x_3 and x_5 represent the displacements of the electromagnet locations, M_0 is the rotor mass matrix, and K_0 is the rotor stiffness matrix.

B. Actuator Dynamics

The attractive force due to an electromagnet is given by the expression

$$P = \frac{A}{\mu_0}B^2 = \frac{A}{\mu_0}\left[\frac{N(i_0+i)}{\frac{l}{\mu}+\frac{x_0+x}{\mu_0}}\right]^2 \tag{2}$$

Manuscript received October 2, 1995; revised April 11, 1996.

The authors are with Chiba University, 1-33 Yayoi-cho, Inage-ku, Chiba 263 Japan.

Publisher Item Identifier S 1063-6536(96)06630-4.

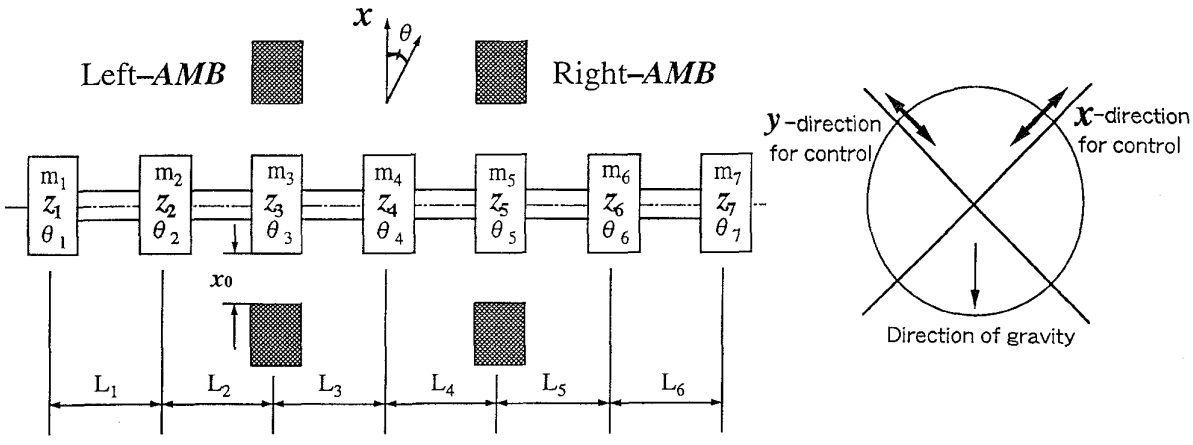

Fig. 1. Model of flexible rotor-magnetic bearing system.

where P is the attractive force, μ_0 is the permeability of free space, A is the air gap area of one pole, B is the magnetic flux density, N is the number of winding turns, i_0 is the bias current, x_0 is the nominal gap length, i is the control current, x is the rotor displacement, l is the length of the ferro magnetic path, and μ is the permeability of the bearing iron. Using Taylor series expansion for small values of i and x, we obtain the following attractive force with linear terms:

$$P \cong p_0 - k_1 x + k_2 i = p_0 + p \tag{3}$$

where

$$k_1 = \frac{2AN^2 i_0^2}{\mu_0^2\left(\frac{1}{\mu} + \frac{x_0}{\mu_0}\right)^3} = \frac{2p_0}{\mu_0\left(\frac{l}{\mu} + \frac{x}{\mu_0}\right)}$$

$$k_2 = \frac{2AN^2 i_0}{\mu_0\left(\frac{l}{\mu} + \frac{x_0}{\mu_0}\right)^2} = \frac{2p_0}{i_0}$$

and p_0 is the bias attractive force. Considering the pair of attractive forces, the magnetic force P due to the electromagnet along the radial direction X can be modeled as the following equation:

$$P' = P_1 - P_2 = -2k_1 x + 2k_2 i \tag{4}$$

where P_1 and P_2 are the top and bottom magnetic forces, respectively. Equation (4) expresses the net actuator force.

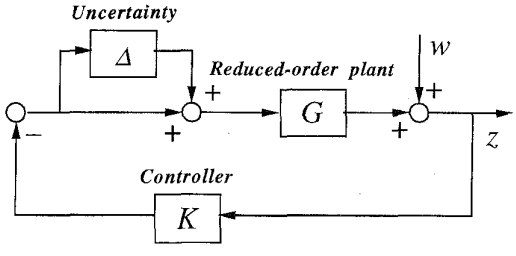

Fig. 2. Plant and closed-loop system having multiplicative uncertainty.

C. Plant Dynamics

The flexible rotor shown in Fig. 1 is acted upon by the attractive forces given in (4). This results in

$$M_0\ddot{q} + K_0 q = Fp' + D \tag{5}$$

where

$$F = \begin{bmatrix} 0 & 0 & 0 & 0 & 1 & 0 & 0 & 0 & 0 & 0 & 0 & 0 & 0 & 0 \\ 0 & 0 & 0 & 0 & 0 & 0 & 0 & 0 & 1 & 0 & 0 & 0 & 0 & 0 \end{bmatrix}^T$$

$p' = [p'_L \quad p'_R]^T$

$P'_l = 2k_1 x_3 - 2k_2 i_l$: forces of the left AMB

$P'_r = 2k_1 x_5 - 2k_2 i_r$: forces of the right AMB

and D represents forces due to the parameter uncertainty and external disturbance.

The bias attractive forces and the control forces in (5) can be separated as follows:

$$M_0\ddot{q} + Kq = F_i i + D \tag{6}$$

where we have the equation shown at the bottom of the page.

$$i = [i_l \quad i_r]^T \qquad K = K_0 + K_i$$

$$K_i = \text{diag}\,(0 \quad 0 \quad 0 \quad 0 \quad -2k_1 \quad 0 \quad 0 \quad 0 \quad -2k_1 \quad 0 \quad 0 \quad 0 \quad 0 \quad 0)$$

$$F_i = \begin{bmatrix} 0 & 0 & 0 & 0 & -2k_2 & 0 & 0 & 0 & 0 & 0 & 0 & 0 & 0 \\ 0 & 0 & 0 & 0 & 0 & 0 & 0 & 0 & -2k_2 & 0 & 0 & 0 & 0 & 0 \end{bmatrix}^T$$

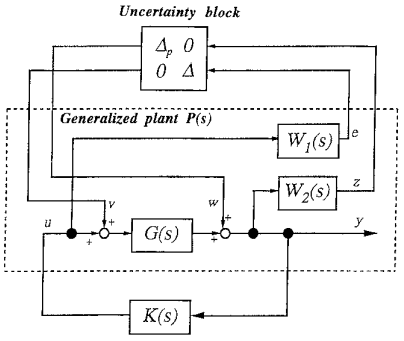

Fig. 3. Block diagram of generalized plant, controller, and uncertainty for μ synthesis.

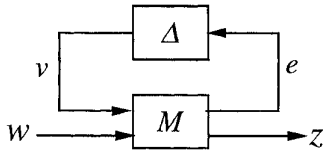

Fig. 4. Equivalent block diagram with linear fractional transformation.

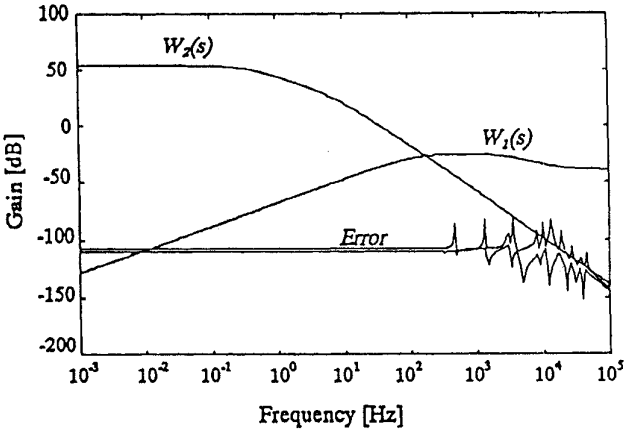

Fig. 5. Frequency weighting functions and error.

Using the modal analysis technique, we can choose the following normalized modal matrix

$$q = \Psi\xi. \tag{7}$$

Equation (6) can now be transformed to the following form in modal coordinates:

$$\ddot{\xi} + \Lambda\dot{\xi} + \Omega^2\xi = f_i i + d \tag{8}$$

where

$$I = \Psi^T M \Psi \quad \Omega^2 = \Psi^T K \Psi \quad \Lambda = 2\zeta Q$$
$$f_i = \Psi^T F_i \quad d = \Psi^T D$$

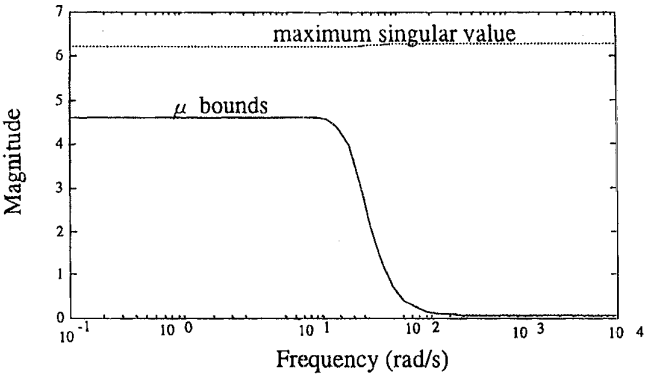

Fig. 6. Maximum singular value and μ bounds of H^∞ controller.

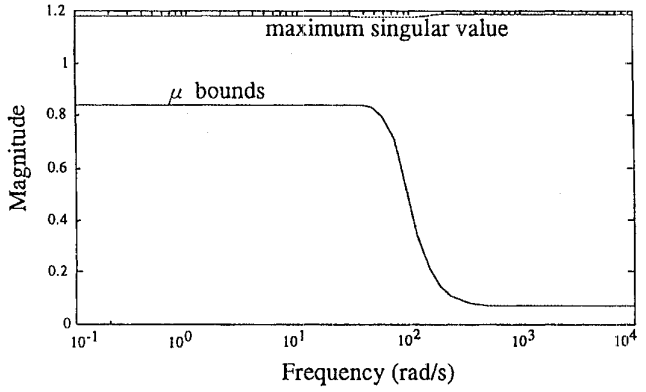

Fig. 7. Maximum singular value and μ bounds of μ_1 controller.

and where Λ is the damping matrix. The damping ratio ζ is determined empirically. The state equation of the electromagnetic-mechanical system is given by

$$\dot{x}_f = A_f x_f + B_f u + D_f \tag{9}$$

where

$$x_f = [\xi \quad \dot{\xi}]^T \quad u = [i_l \quad i_r]^T$$
$$A_f = \begin{bmatrix} 0 & I \\ -\Omega^2 & -\Lambda \end{bmatrix} \quad B_f = \begin{bmatrix} 0 \\ f_i \end{bmatrix} \quad D_f = \begin{bmatrix} 0 \\ d \end{bmatrix}.$$

If the rotor displacement is measured at the magnetic bearings, the output equation is

$$y = C_f x_f = [x_3 \quad x_5]^T \tag{10}$$

where

$$C_f = [F_i^T \Psi \quad 0].$$

D. Reduced-Order Model

Because this MIMO system is originally unstable in an open loop, the control objective is to levitate the rotor and achieve stability. In this case, there are only two unstable rigid modes, and all of the flexible modes are stable. Since

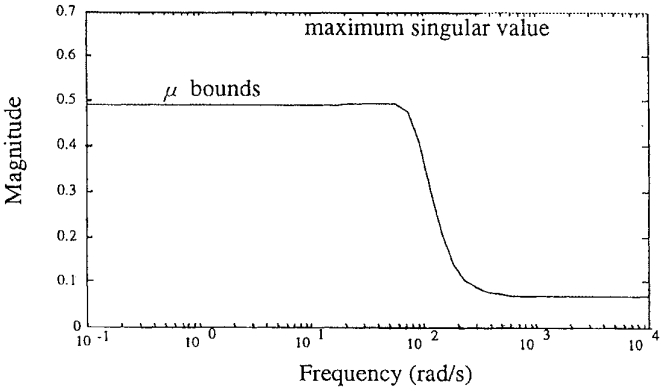

Fig. 8. Maximum singular value and μ bounds of μ_2 controller.

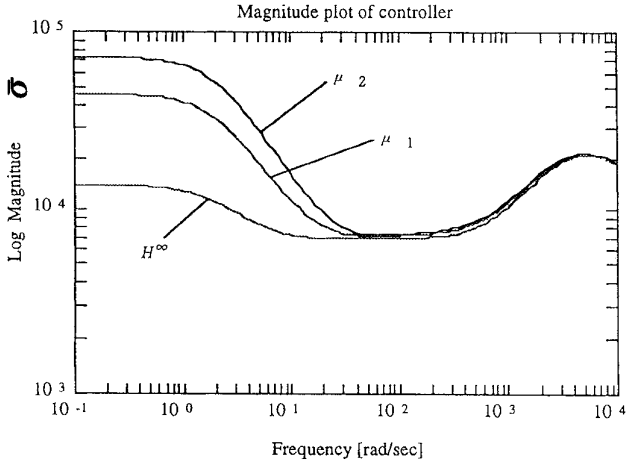

Fig. 9. Frequency response of H^∞, μ_1, μ_2 controllers.

it is difficult to design and execute a controller based upon a high-order model of a flexible system, the construction of a reduced-order model is highly desirable. Here, a reduced-order model is constructed by truncation of the higher order modes in modal coordinates. In this case, the state equation and the output equation including the ith order mode may be written as follows:

$$\begin{aligned} \dot{x}_r &= A_r x_r + B_r u + D_r \\ y &= C_r x_r = [x_3 \quad x_5]^T \end{aligned} \tag{11}$$

where

$$x_r = [\xi_1, \xi_2, \cdots, \dot{\xi}_i \xi_1, \dot{\xi}_2, \cdots, \dot{\xi}_i]^T.$$

From the standpoint of stabilizing the rigid body modes, we may consider a reduced-order model in which not only the rigid body modes but also the first bending mode are retained [$i = 3$ in (11)]. In addition, the closed-loop system must maintain the robust stability without spillover caused by ignored high-frequency modes.

III. μ Synthesis Theory

The background, framework, and control system design procedure of μ synthesis are given in [3], [4], and [13].

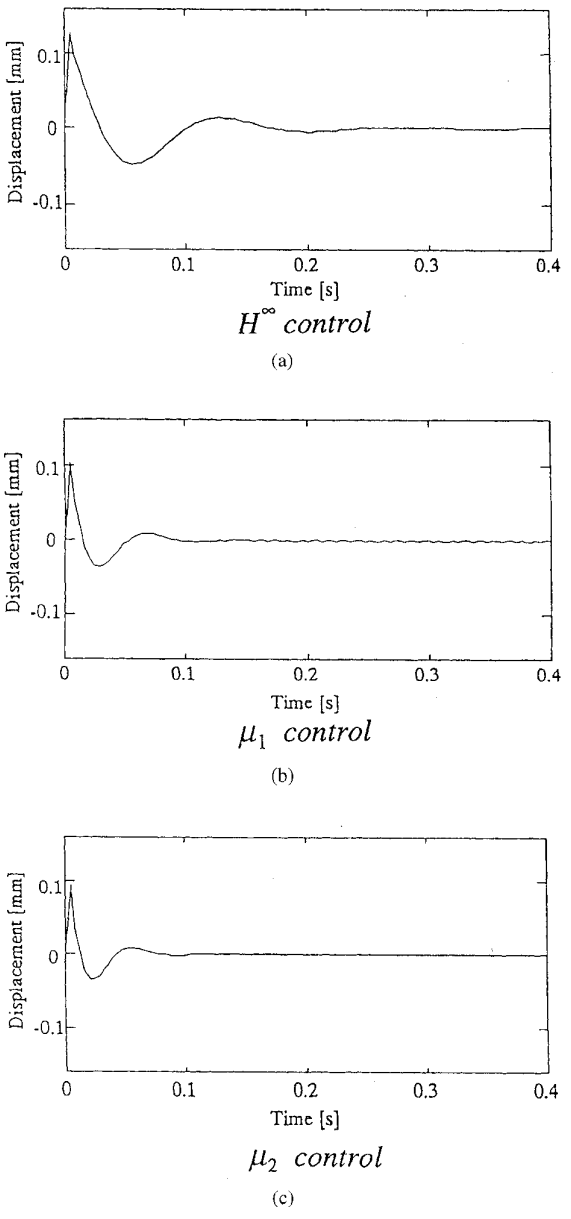

Fig. 10. Simulated impulse response.

Consider a model which has multiplicative uncertainty as indicated in Fig. 2. Regardless of whether the uncertainty is on the output side or on the input side, the same situation is obtained except that the order of the multiplication of G and K is changed. In H_∞ control, the stability conditions are based on the small gain theorem. In this case, the maximum singular value of Δ is limited and the structure of Δ is a full complex matrix. That is, there are uncertainties even among nondiagonal elements. The weighting function for the robust stability of the mixed sensitivity problem tends to be larger than necessary. Moreover, in the nominal performance, no uncertainties are taken into consideration in the performance. These two problems may be said to be problem of H_∞ control.

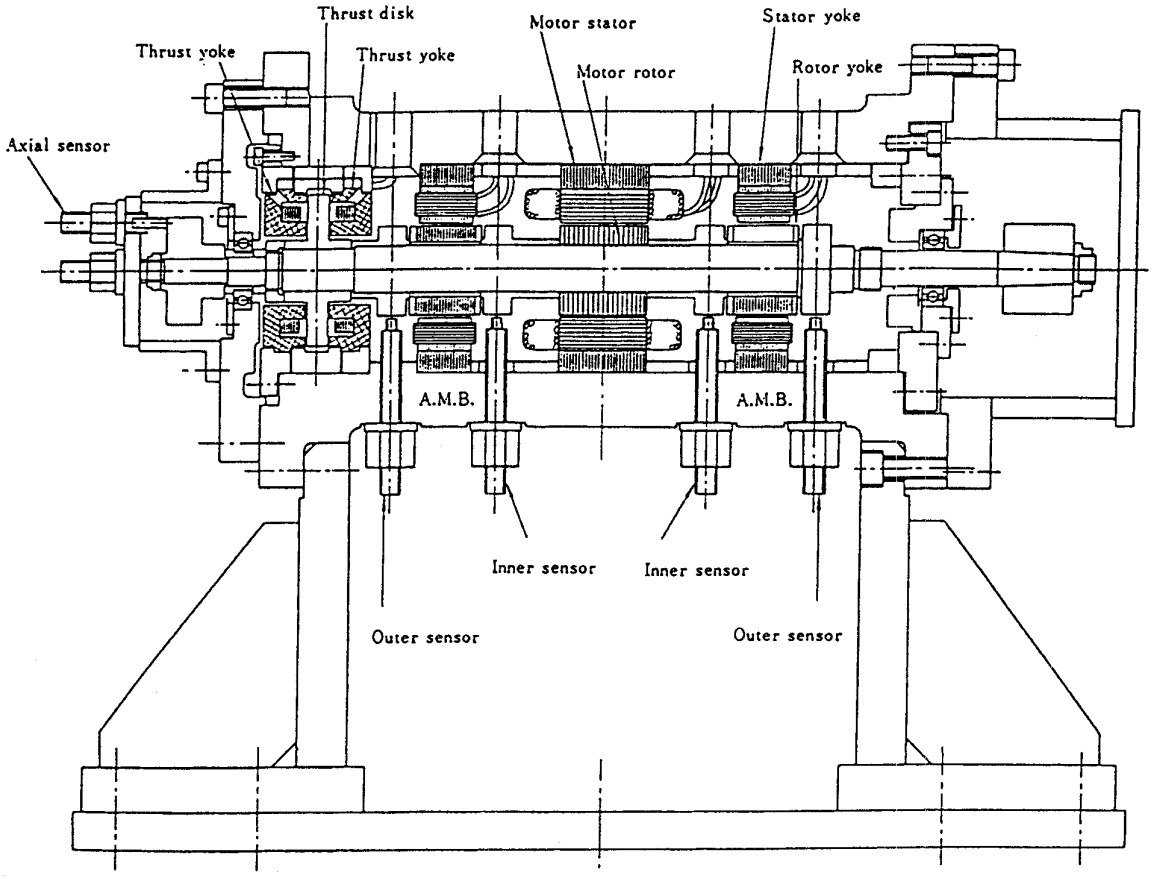

Fig. 11. Rotor test rig.

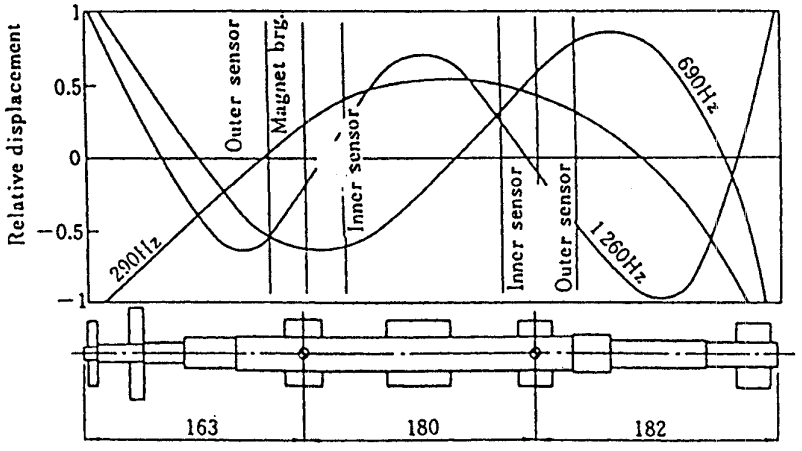

Fig. 12. Rotor modeshapes and natural frequencies with indicated bearing and sensor locations.

In μ synthesis, the design problem is as shown in Fig. 3. The μ synthesis framework consider a system with structured uncertainty Δ and attempts to find a μ controller which achieves robust stability, nominal performance, and robust performance simultaneously. Fig. 3 can be rearranged to yield Fig. 4. In this case, M is given as

$$M = \begin{bmatrix} W_1T & W_1KS \\ W_2SG & W_2S \end{bmatrix} = \begin{bmatrix} M_{11} & M_{12} \\ M_{21} & M_{22} \end{bmatrix} \tag{12}$$

where

$$S = (I + GK)^{-1}, \quad T = GK(I + GK)^{-1} \tag{13}$$

are given. From (12), the transfer function from v to e is W_1T, which is precisely the robust stability condition itself, namely

$$||W_1T||_\infty < 1. \tag{14}$$

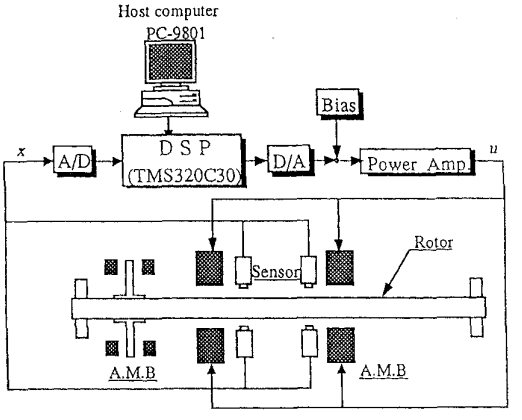

Fig. 13. Configuration of DSP-based control system.

TABLE I
PARAMETER VALUES

Parameter		Value	Parameter		Value
Mass	m_1	0.03 kg	Diameter	d	0.0275 m
	m_2	0.15 kg	Gap	x_0	0.0003 m
	m_3	1.0 kg	Bias current	i_0	3.0 A
	m_4	0.5 kg	Bias attractive force	p_0	100.0 N
	m_5	1.0 kg			
	m_6	0.0 kg			
	m_7	0.09 kg	Damping ratio (i=1, ···,14)	ζ_i	0.001
Length	L_1	0.09 m			
	L_2	0.072 m	Permeability of magnet iron	μ	$2\pi \times 10^3$
	L_3	0.09 m			
	L_4	0.09 m			
	L_5	0.091 m	Permeability of free space	μ_0	$4\pi \times 10^7$
	L_6	0.091 m			

In addition, the transfer function from w to z is W_2S, which is nothing but the nominal performance itself, namely

$$||W_2S||_\infty < 1. \tag{15}$$

In point of fact, μ synthesis is not only achieves these two performances but also imposes the following condition as robust performance:

$$\sup_{\overline{\sigma}(\Delta)\leq 1} ||F_u(M,\Delta)||_\infty \leq 1. \tag{16}$$

Here, F_u is the linear fractional transformation and is defined by

$$F_u(M,\Delta) = M_{22} + M_{21}\Delta(I - M_{11}\Delta)^{-1}M_{12}. \tag{17}$$

However, it is virtually impossible to find conditions that will satisfy (16). Therefore, consider the following expression instead of (16):

$$\mu_\Delta(M) < 1 \tag{18}$$

where, $\mu_\Delta(M) < 1$ is defined by

$$\mu_\Delta(M) = \frac{1}{\min\{\overline{\sigma}(\Delta): \Delta \in \Delta, \det(I - M\Delta) = 0\}}. \tag{19}$$

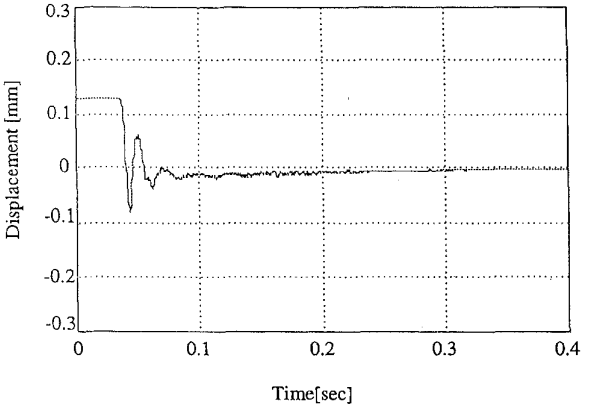

(a)

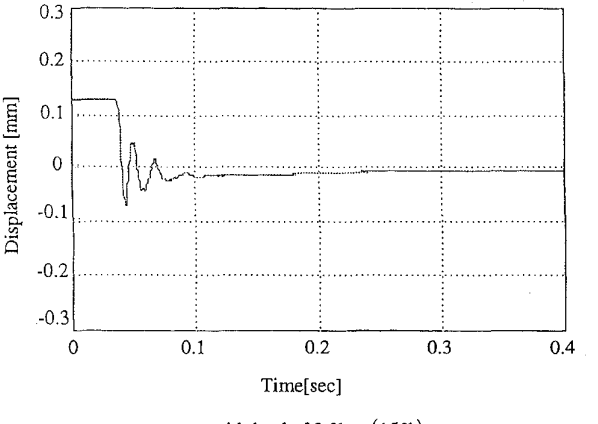

(b)

Fig. 14. Levitation time history with H^∞ control, two-axis control.

$\mu_\Delta(M)$ is called a structured singular value. The denominator of (19) indicates the smallest perturbation that causes "instability" in the constant matrix feedback loop. As the structured singular value is inverse, as shown in (19), the smaller μ means that the limit of destabilization increases for parameter variations, and the closed-loop system provides stronger robust performance. It is known that $\mu_\Delta(M)$ has the following relation:

$$\max \rho(QM) \leq \mu_\Delta(M) \leq \inf \overline{\sigma}(DMD^{-1}) \tag{20}$$

where D is the scaling matrix. Since $\mu_\Delta(M)$ cannot typically be computed, we calculate the upper bound $\inf \overline{\sigma}(DMD)^{-1}$.

IV. DESIGN OF μ CONTROL SYSTEM

We designed the control system using D-K iteration to find an approximate solution. The fourth-order system is used for control system design as reduced-order model $G(s)$. The rotor has the first bending critical speed at 290 Hz (17 400 r/min) and the second at 690 Hz (41 400 r/min) as shown in Fig. 12. The operating speed of this rotor is about 35 000 r/min (583 Hz) between the first bending mode and

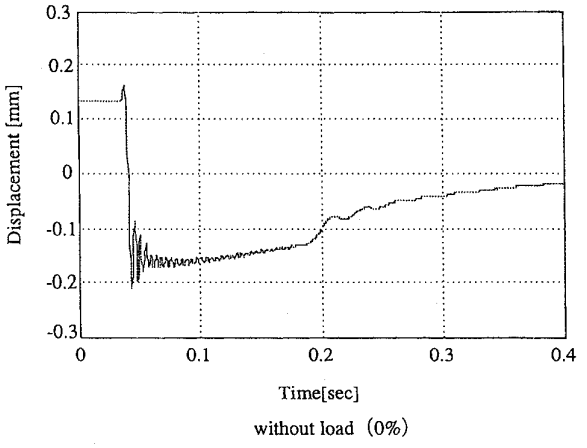

(a)

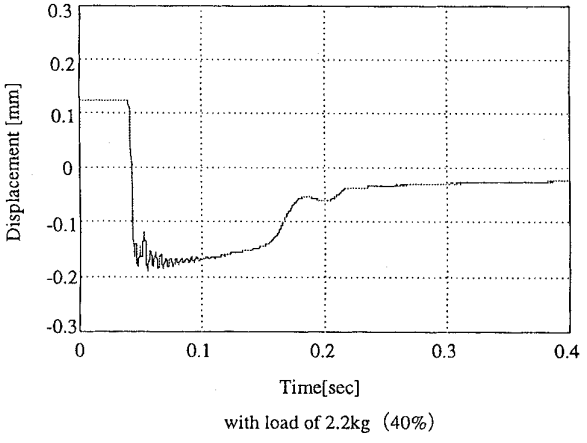

(b)

Fig. 15. Levitation time history with μ_1 control, two-axis control.

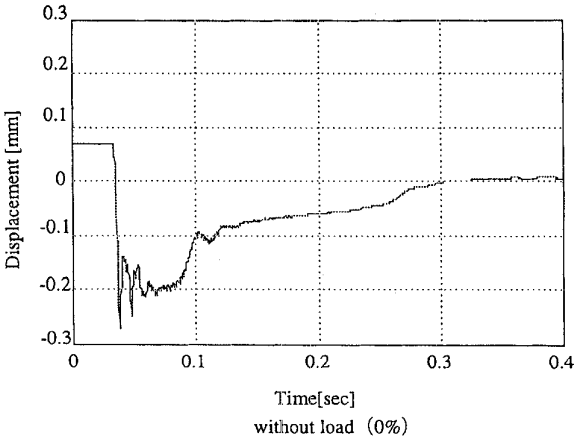

(a)

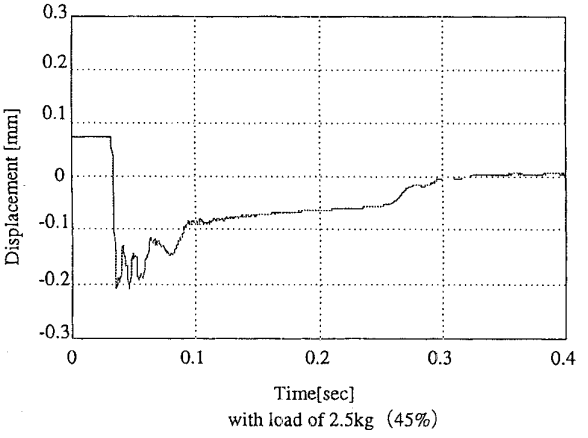

(b)

Fig. 16. Levitation time history with μ_2 control, two-axis control.

the second bending mode. This means this test rotor is a typical flexible rotor. Fig. 5 shows the frequency weighting functions W_1 and W_2 the error introduced by approximating the full-order model by the reduced-order model. We have chosen the weighting functions of and taking into account above mentioned facts. However, a considerable number of "cut and try" iterations were required to pick W_1 and W_2. Using the weighting functions $W_1(s), W_2(s)$ shown in Fig. 5, a 12th-order generalized plant $P(s)$ was determined as shown in Fig. 3, The weighting filters $W_1(s), W_2(s)$ were selected based on the desired controller band width and the frequency of the truncated vibration modes. An H_∞ controller was designed using these weights. Next, we performed μ analysis for the H_∞ controller. Fig. 6 shows a plot of μ versus frequency. The maximum value of μ was 4.6, which implies that robust performance is not achieved as it dose not satisfy (18). The scaling matrices resulting from the μ calculation were fitted over frequency with a constant matrix. The new generalized plant P_2 was constructed so as to include this scaling matrix. The resulting controller is referred to as the μ_1 controller. The plot of μ for this controller is shown in Fig. 7 and the maximum μ is 0.82, therefore robust performance is achieved in this system with the μ controller. Another D-K iteration resulted in the μ_2 controller which achieved an even smaller peak μ value, as shown in Fig. 8. Fig. 9 shows the magnitude plots of the designed controllers. The μ_2 controller has the highest gain in the lower frequency region, so the μ_2 controller is expected to have strong robustness, since the sensitivity of the closed-loop system is reduced at low frequency. Fig. 10 shows the simulated impulse response for the three controllers. The best performance is obtained by a μ_2 controller.

V. Experimental Results

A. Test Rig

The test rig for the magnetic bearing system is shown in Fig. 11 and the parameter values for this rig and its corresponding rotor model are given in Table I. An induction motor rotor is located in the middle of the shaft and two radial magnetic bearings are located on both sides of the motor rotor. A magnetic thrust bearing is located at left end of the shaft. Fig. 12 shows the rotor geometry and the free vibration modes. Fig. 13 shows the configuration of the experimental set up. For our robustness experiments, we can hang weight using wire

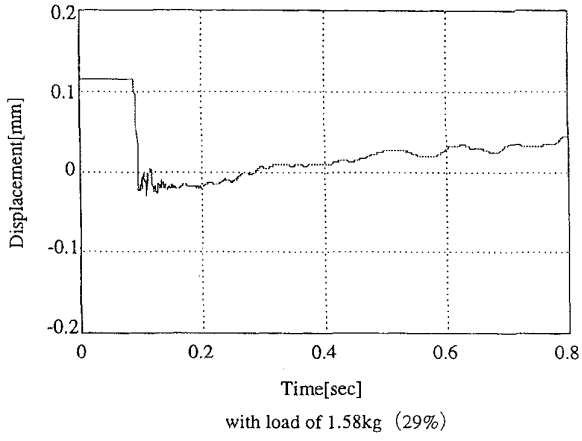

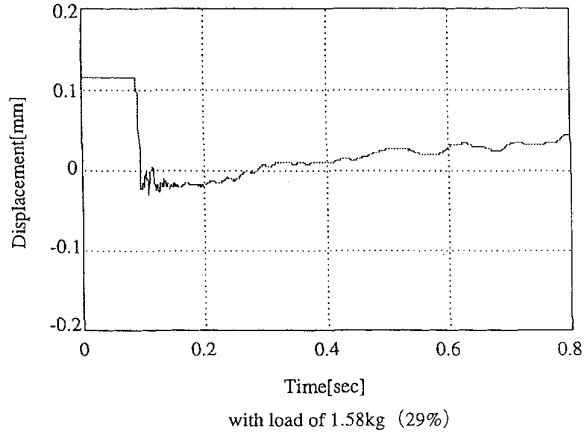

Fig. 17. Levitation time history with H^{∞} control, four-axis control.

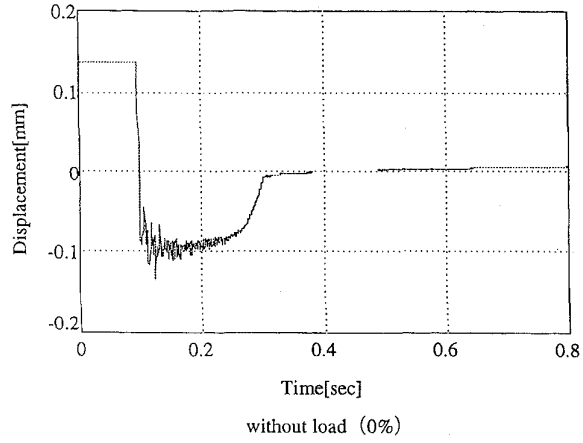

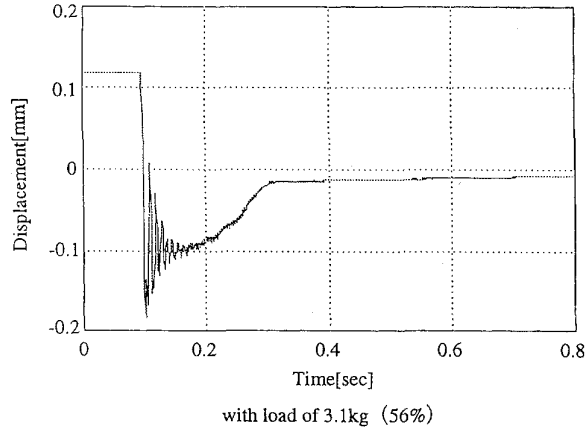

Fig. 18. Levitation time history with μ_1 control, four-axis control.

on the right-hand side end of the rotor. The rotor cannot be rotated with the added mass.

B. Two-Axis Control Experiments

For these tests, the X direction motion was controlled by either the H_∞ or the μ controller, while the Y direction motion was controlled by analog PID control. Figs. 14(a), 15(a), and 16(a) show the nominal levitation time history for the H_∞, μ_1, and μ_2 controllers respectively. It was found that the steady state error was smallest with the μ_2 controller due to a strong integrator action. Figs. 14(b), 15(b), and 16(b) show robust performance of the three controllers for variations in the rotor mass (nominal is 5.5 Kg). The upper stability limits of mass variation are 15% for H_∞, 40% for μ_1 and 50% for μ_2. It can be seen that the closed-loop system with μ_2 controller provides superior stability robustness and rejection of low-frequency disturbances It is not easy to realize similar good performance using a conventional analog compensator.

C. Four-Axis Control Experiments

For the next set of tests, both of the X and Y directions were controlled by DSP-based H_∞ or μ controllers. Figs. 17(a), 18(a), and 19(a) show the levitation time history. The nominal performance shown here is very similar to that in Section V-B. However, the settling after lift-off for the μ_2 controller takes twice the time required in the two-axis case. This is, in fact, longer than the levitation. Therefore, the nominal performance in the μ control system presented here is inferior in terms of setting time in comparison to the analog PID control system. Next, the robust performance of the three controllers was examined. Figs. 17(b), 18(b), and 19(b) show the levitation time histories for the three controllers when the mass is increased to its upper stability limit. The upper limits of the mass variation from the nominal value are 29% for H_∞, 56% for μ_1 and 73% for μ_2. We believe that the four axis control displays greater robustness because the PID controller used in the two axis tests are not as robust to the added mass. These μ controllers were designed as a continuous-time compensator at first, and then transformed to a discrete-time compensator for implementation on the DSP using a bilinear transformation. If these compensators were directly designed as a discrete-time compensator, performance could be improved even more. These results are qualitatively similar to

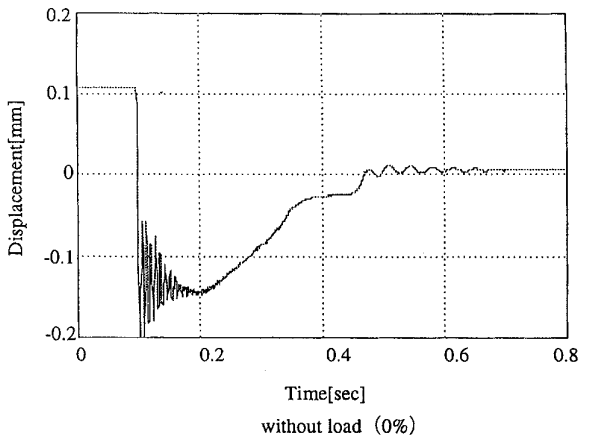

(a)

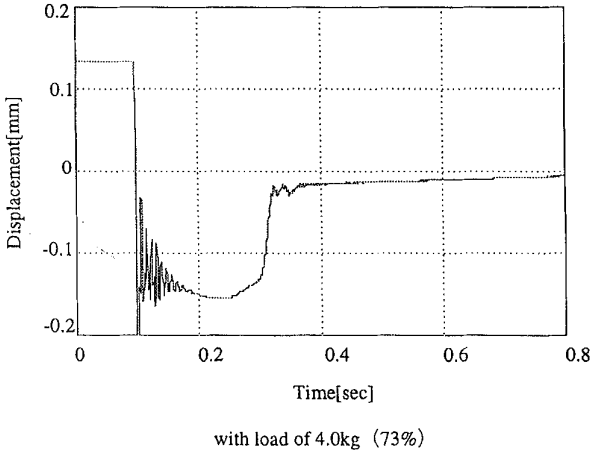

(b)

Fig. 19. Levitation time history with μ_2 control, four-axis control.

the simulation results. Fig. 20 shows the experimental impulse responses corresponding to Fig. 10. These results are also qualitatively in good agreement with the simulations results. We carried out the rotation test up to 35 000 r/min for the nominal rotor (without added mass). In cases of the rotation test, we observed nearly the same performance for the H_∞, μ_1, and μ_2 controllers.

VI. Conclusions

In this paper, we applied μ synthesis theory to problem of designing controllers for flexible rotor/magnetic bearing systems. In simulations and experiments the μ control system provided greater stability robustness and rejection of low-frequency disturbances than H_∞ control. Our conclusions are summarized as follows:

1) Stabilization of a rotor in active magnetic bearings can be realized with high stiffness by controllers designed via μ synthesis.
2) The μ controllers exhibited much greater stability robustness than H_∞ control to variations in rotor mass.
3) Decreasing the structured singular value μ via D-K iteration is very important to achieving good robust performance, as shown by the test of the μ_1 and μ_2 controllers.

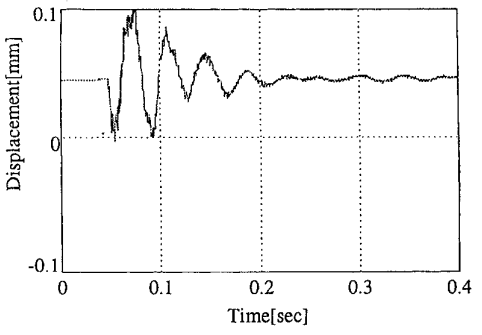

(a)

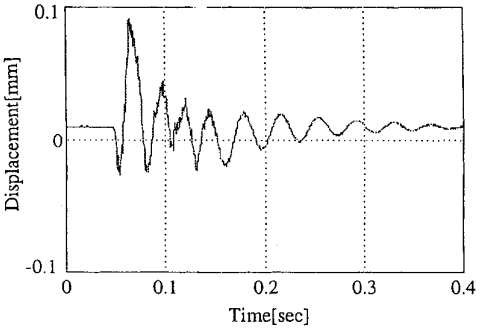

(b)

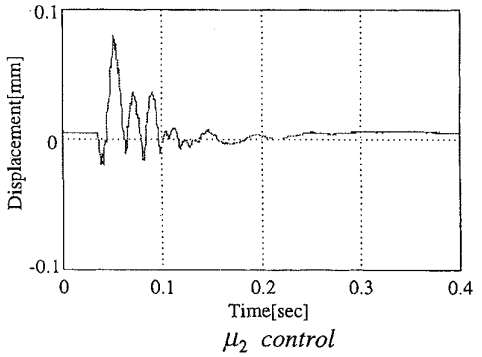

(c)

Fig. 20. Experimental impulse responses.

Acknowledgment

The authors gratefully acknowledge the support of Ebara Research Co. Ltd. of Japan for providing the experimental setup.

References

[1] M. Green and D. J. N. Limebeer, *Linear Robust Control*. Englewood Cliffs, NJ: Prentice-Hall, 1994.
[2] K. Zhou, J. Doyle, and K. Glover, *Robust and Optimal Control*. Englewood Cliffs, NJ: Prentice-Hall, 1995.

[3] J. Doyle, A. Packard, and K. Zhou, "Review of LFT's, LMI's, and μ," in *Proc. 30th IEEE Conf. Decision Contr.*, 1991, pp. 1227–1260.
[4] G. Balas, J. Doyle, K. Glover, A. Packard, and R. Smith, *μ Analysis and Synthesis Toolbox User's Guide*. Minneapolis, MN: Musysn, 1991.
[5] V. I. Utkin, *Sliding Modes in Control Optimization*. New York: Springer-Verlag, 1992.
[6] A. S. I. Zinober, Ed., *Variable Structure and Lyapunov Control*. New York: Springer-Verlag, 1994.
[7] K. Nonami and H. Tian, *Sliding Mode Control*. Tokyo, Japan: Corona (in Japanese), 1994.
[8] W. Cui and K. Nonami, "H_∞ control of flexible rotor-magnetic bearing systems," in *Proc. 3rd Int. Symp. Magn. Bearings*, 1992, pp. 505–512.
[9] K. Nonami and H. Yamaguchi, "Robust control of magnetic bearing systems by means of sliding mode control," in *Proc. 3rd Int. Symp. Magn. Bearings*, 1992, pp. 537–548.
[10] K. Nonami, H. Ueyama, and Y. Segawa, "H_∞ control of milling AMB spindle," in *Proc. 4th Int. Symp. Magn. Bearings*, 1994, pp. 531–536.
[11] H. Tian and K. Nonami, "Robust control of flexible rotor-magnetic bearing systems using discrete-time sliding mode control," in *Proc. 4th Int. Symp. Magn. Bearings*, 1994, pp. 47–52.
[12] ——, "Discrete-time sliding-mode control of flexible rotor-magnetic bearing systems," to appear in *J. Robust Nonlinear Contr.*, 1996.
[13] J. Doyle, "Analysis of feedback systems with structured uncertainty," *Proc. IEEE*, vol. 129, pp. 242–250, 1982.
[14] M. Fujita, F. Matsumura, and T. Namerikawa, "μ analysis and synthesis of a flexible beam magnetic suspension system," in *Proc. 3rd Int. Symp. Magn. Bearings*, 1992, pp. 495–504.
[15] M. Fujita, K. Hatake, F. Matsumura, and K. Uchida, "An experimental evaluation and comparison of H_∞/μ control for a magnetic bearing," in *Proc. 12th IFAC World Congr.*, vol. 4, 1993, pp. 393–398.

Kenzo Nonami received the Ph.D. degree from Tokyo Metropolitan University in 1979.

He was named a Professor in the Department of Mechanical Engineering at Chiba University, Japan, in December 1994. He worked at Chiba University as a Research Associate from 1980 to 1988, and as an Associate Professor from 1988 to 1994. He was a NASA NRC Research Associate from 1985 to 1986 and also in 1988. His current research interests include active vibration control for flexible structures, active control for magnetic bearings and magnetic levitations, control for locomotion robots and space robots, active noise control, robust control theory, and their applications.

Takayuki Ito was born in Saitama, Japan, in 1972. He received the B.E. and M.E. degrees in mechanical engineering from Chiba University, Japan, in 1994 and 1996, respectively. He is currently completing the Ph.D. degree at Chiba University.

His research interests include sliding mode control with frequency shaping and its applications.